Journal of Materials Science and Chemical Engineering, 2016, 4, 8-21
Published Online February 2016 in SciRes. http://www.scirp.org/journal/msce
http://dx.doi.org/10.4236/msce.2016.42002

Fabrication of UO_2-Gd_2O_3 Fuel Pellets

Balakrishna Palanki

Nuclear Fuel Complex, Hyderabad, India
Email: palankibalakrishna@yahoo.com

Received 15 November 2015; accepted 28 January 2016; published 1 February 2016

Abstract

The burnable poison Gadolinium oxide was incorporated into UO_2 in two of the 36 elements of the fuel assembly in the reload fuel of BWR Units I & II of Tarapur Atomic Power Station. This enabled loading of higher quantities of fuel and achieving a more flattened neutron flux distribution over a longer period of time in the nuclear reactor core. The UO_2-Gd_2O_3 pellets are made by powder pressing and sintering. In the early days of this author's experience of the 1970s, the processing of UO_2-Gd_2O_3 turned out to be more complex than that of UO_2 alone. The small proportion of Gd_2O_3 in the powder mixture (1.5%) is to be uniformly distributed in the UO_2 before and after sintering and substitutional solid solution formation must be complete prior to densification. The inadequacy of homogeneity in the powder and pressed pellets leads to severe defects in the sintering process. In this paper, the processing of UO_2-Gd_2O_3 has been revisited. The defects in the product such as "free gadolinia", low sintered density and bloating, caused by improper processing, have been brought out. The structural defect chemistry aspects of UO_2-Gd_2O_3 and diffusion processes relevant to sintering have also been discussed.

Keywords

UO_2-Gd_2O_3, Compaction, Sintering, Defects, Structural Chemistry, Diffusion

1. Introduction

The Boiling Water Reactor 1 fuel assembly used in TAPS I and II consisted of 36 fuel rods in 6 × 6 square array using three enrichments of ^{235}U, namely 1.6%, 2.1% and 2.66% in 3, 11 and 22 rods respectively, in the form of sintered UO_2 pellets. Two of the 2.66% enriched rods contained 1.5% by weight of Gd_2O_3 the balance being UO_2. This author was responsible for the production of required quantities of UO_2-Gd_2O_3 pellets in the 1970s. A part of the experience accrued was described in publications at the time and in course of time after the tenure [1]-[8]. However, these publications are not readily accessible to the manufacturing community now as they belong to the era before internet. This paper revisits the experiences of the time. Some of the aspects that were missed at that time as well as new insights acquired later in the light of newly available literature are also in-

How to cite this paper: Palanki, B. (2016) Fabrication of UO_2-Gd_2O_3 Fuel Pellets. *Journal of Materials Science and Chemical Engineering*, **4**, 8-21. http://dx.doi.org/10.4236/msce.2016.42002

cluded here with the benefit of hind sight.

2. Powder Mixing

Some characteristics of UO_2 powder and Gd_2O_3 powder received from supplier "B" are given in **Table 1**.

Initially, the double cone mixer was used for mixing Gd_2O_3 and UO_2 powders. However, the major constituent UO_2 powder turned out to be not free flowing. Hence, a ribbon mixer was used in place of the double cone mixer with improved results [1]. In a double cone, the mixing takes place by shearing of particle layers over one another as the double cone rotates and hence suitable for mixing free flowing powders. In the ribbon mixer, mixing takes place by convection and hence suitable for powders that do not flow freely. As the specified Gd_2O_3 content was only 1.5%, first a master mix containing about 30% Gd_2O_3 was made which was diluted by adding UO_2 in a second mixing operation. In the final mixed powder, 5 g samples were drawn and analyzed for Gd_2O_3 content. The sample was analyzed by gravimetric procedure. The UO_2-Gd_2O_3 powder of about 5 g (accurately weighed on an analytical balance with an accuracy of ±0.0001 g) was dissolved in nitric acid. The U was separated by solvent extraction. The Gd remaining in the raffinate solution was precipitated by oxalic acid and the residue retained on the filter paper after the filtration was ignited and weighed as Gd_2O_3. The Gd_2O_3 contents determined this way in various lots are plotted for each mixer and are shown in **Figure 1**.

Denoting the mean and standard deviation of the frequency distribution as μ and σ respectively, the efficiency of mixing may be defined as

$$\eta_{mean} = \left[1 - \left|G - \mu\right| / G\right] 100$$

Table 1. Comparison of UO_2 and Gd_2O_3 powders.

Property	UO_2	Gd_2O_3
APS Fisher sub sieve sizer, μm	0.8 − 1.0	0.5 − 1.0
BET specific surface area, m^2/g	2.5 − 3.2	3.9 − 9.1
Tap density, g/cm^3	2.2 − 2.8	0.8 − 1.3
Theoretical density, g/cm^3	10.96	7.41
Flowability	Poor	Nil
Appearance	Fine particles, separable	Agglomerated
Dry sieve analysis	100% passes through 100 mesh	Forms agglomerates in sieving
Melting point, ˚C	2800	2420
Crystal structure	Face centered cubic	Cubic, monoclinic
Phase change temperature, ˚C	No phase change	1200
Range of nonstoichiometry	Wide	Narrow

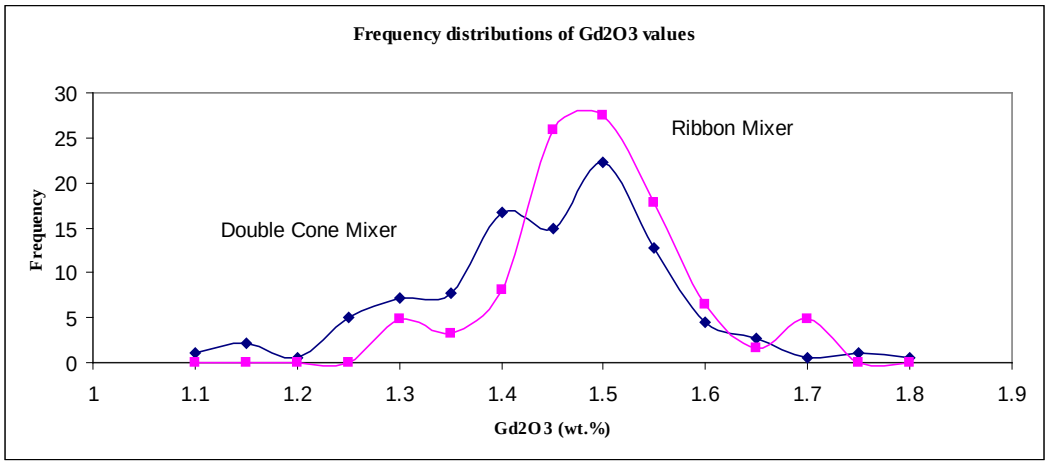

Figure 1. Frequency distributions of Gd_2O_3 values from analytical samples from different mixers, using data from [2].

where G is the Gd_2O_3 added and μ is the mean of the statistical distribution of Gd_2O_3% values from analytical samples drawn from the powder mixture from different lots of powder over a period of time.

We may define efficiency of mixing (η_{sd}) based on standard deviation as $\eta_{sd} = \left[\left(2/\Pi\right)\cot^{-1}\sigma\right]100$, where $\cot^{-1}\sigma$ is in radians, or $\eta_{sd} = \left[\left(1/90\right)\cot^{-1}\sigma\right]100$, where $\cot^{-1}\sigma$ is in degrees.

The required level efficiencies were arrived at on the basis of the internal control limits of 1.45 and 1.55 Gd_2O_3% in the powder mixture. For the types of powder used, the ribbon mixer is seen to be a little more efficient than the double cone blender, as shown in **Table 2**. Both the machines are satisfactory with respect to mean but not so with respect to standard deviation. The ribbon mixer was operated intermittently, to prevent possible oxidation of UO_2 powder from the friction heat from the blades.

3. Powder Milling

Initially, Gd_2O_3 powder was obtained from one supplier, let us say, "Supplier A". Subsequently, another source was identified, let us say, "Supplier B". Two problems cropped up: 1) Unacceptable "islands" of undissolved Gd_2O_3 were found in the ceramographs of sintered UO_2 matrix, termed "free gadolinia". The free gadolinia was more than that specified [9] [10] for sintered pellets. 2) Low sintered density and bloating were noticed in some lots of sintered pellets. Both the problems were traced to the second supply of the powder. While the powder from "A" was crystalline and flowed freely, that from "B" was less crystalline, had a greater BET specific surface area, had higher moisture content, was nonflowable and agglomerated easily. The agglomerates of Gd_2O_3 did not break up into smaller entities in the mixing process.

Simple mixing of Gd_2O_3 with UO_2 powder led to defective pellet sections containing undissolved or "free" Gd_2O_3. Hence a light milling step became necessary for the master mix to achieve de-agglomeration and improved dispersion of Gd_2O_3 in UO_2. Smaller islands of Gd_2O_3 in the green UO_2 matrix means smaller diffusion distances during dissolution and sintering [2].

The term 'Milling' here is not the same as that used in 'Mining and milling' in the context of the Nuclear Fuel Cycle. It is simply a particle size reduction process carried out using a ball mill or a hammer mill or a rod mill or a jet mill or an attritor.

In the case of UO_2-Gd_2O_3 powder as well as UO_2 powder not containing Gd_2O_3, the light milling step was found to have modified the powder characteristics by breaking down the agglomerates and enhancing the packing efficiency in the compaction die. Higher green densities were achieved at lower compaction pressures. Pellets of higher sintered densities and minimum chipping and cracking resulted with greater acceptance levels at the Quality Control department.

4. Low Sintered Density and Bloating

The specified sintered density was 93% to 97% TD. In some of the lots, the sintered pellets were found to be of lower density. TiO_2 is known to be a sintering aid for UO_2 [11] [12]. It was therefore added to the powder mixture of UO_2-Gd_2O_3 with the aim of improving sintered density. However, not only there was no improvement of density, but in some cases the density decreased further. In some pellets, bloating was noticed. Sections of the low density sintered pellets exhibited large voids of various sizes in the range 30 to 160 μm. The larger and more extensive the voidage, the lower was the sintered density.

The clue to our low density and bloating problems came from literature on stable density fuel [2]. Fine voids remnant in the fuel after sintering were found to close during fuel irradiation causing unwanted in-reactor fuel densification and consequent shrinkage of the fuel. The driving force for void closure depended on its size and nature and extent of gases trapped in the voids. Though the small radial shrinkage is not serious in a free standing design of the fuel element, this was not the case with axial shrinkage. As a result, the fuel column shifted

Table 2. Comparison of efficiencies mixing machines.

	Number of samples	η_{mean}	η_{sd}
Double cone Mixer	180	96.0	92.4
Ribbon Mixer	62	99.3	94.5
Required	–	96.7	96.8

downward in the fuel element. The axial gap so formed had propensity to collapse under cooling water pressure. In the concept of stable density fuel, pore formers were incorporated in the powder before pressing, so that stable voids remained in the fuel and the prospect of in reactor fuel densification could be avoided [13]-[15].

The sintering characteristics of the UO_2-Gd_2O_3 pellets depend on the size and dispersion of Gd_2O_3 particles in the UO_2 matrix of the green pellet, in the case where the Gd_2O_3 powder is mixed by mechanical means. In our processing, the Gd_2O_3 agglomerates in UO_2 matrix behaved as unintended pore formers which caused remnant porosity in the sintered pellets. The Gd_2O_3 dissolves in the UO_2 during sintering much before densification is complete. The space originally occupied by the Gd_2O_3 agglomerate in the green pellet is vacated by its dissolution and diffusion into Gd_2O_3. Whether the void thus left over shrinks to closure during further sintering or remains stable or grows depends on its size. Large agglomerates of UO_2-Gd_2O_3 were found to leave large voids (of over 30 μm) that led to either low density or bloating. The problem was solved to a great extent by light dry milling the mechanical mixtures. The dry milling operation resulted in breaking of the agglomerates to smaller sizes, leading to smaller voids that could readily close in the sintering process. The milling has to be mild in order to avoid possible contamination from grinding media, possible heat generation leading to oxidation of UO_2 to U_3O_8 and for radioactive dust containment. Wet milling could not be considered under the Plant circumstances.

To verify the hypothesis that the void space left over after the Gd_2O_3 agglomerate dissolved was responsible for the low density, an experiment was performed wherein, Gd_2O_3 powder granules of known size (obtained by sieving) were mixed with UO_2 powder, compacted and sintered. The results are given in **Table 3**.

Potter and Davis found that as little as 0.5 wt.% of Gd_2O_3 reduced the sinterability [16]. Song *et al*. found that as the oxygen potential of sintering atmosphere increases, the density of the UO_2-2%Gd_2O_3 increases, but that of UO_2-10%Gd_2O_3 pellets decreases [17]. They also found that Gd ions diffused in to UO_2, but U ions did not diffuse into Gd_2O_3 when a diffusion couple of UO_2/Gd_2O_3 was annealed at 1700˚C for 100 hours in hydrogen gas due to Kirkendall effect. They determined sintered density of UO_2-10%Gd_2O_3 as a function of CO_2 to H_2 volume ratio in the sintering atmosphere. The density decreased from 91%TD to about 88.6% TD as the CO_2/H_2 was increased from 0.05 to 0.30. The driving force for pore closure was expected to be much smaller in an oxidizing atmosphere than in a reducing atmosphere [18].

Nishida and Yuda [19] prepared UO_2/Gd_2O_3 diffusion couple. They heated one couple at 1700˚C for 100 hours and another at 1800˚C for 100 hours in an atmosphere of 92% N_2 + 8% H_2 gas with a dew point of 21˚C. They evaluated the effective inter−diffusion coefficient and found it to be smaller than grain boundary diffusion coefficient and larger than the volume diffusion coefficient. For normal commercial sintering temperature of 1750˚C and time 4 hours, they estimated an inter−diffusion distance of 2 μm for U ion as well as Gd ion. They also found a decline in the sintered density of UO_2 containing 5% and 10% Gd_2O_3 as the oxygen potential was increased from −410 to −310 kJ/mol. Ho and Radford also found that high density was achieved in dry hydrogen and low densities in commercial fabrication conditions [20].

More recently, Durazzo *et al*. [21] and [22] studied the mechanism of pore formation in UO_2-Gd_2O_3 pellets and they also attributed the porosity to Kirkendall effect, wherein Gd and U have different inter-diffusion rates. They also correlated the pore size with the Gd_2O_3 agglomerate size.

Even without the addition of Gd_2O_3, the density of UO_2 pellets decreased with sintering time caused by pore growth [7] and [23]. Here there is no Kirkendall effect since there is only one species. Chalder observed retarded densification in UO_2 compacts made from spray dried granules. The hard granules could not be broken down in

Table 3. Observed pore size and density of UO_2-1.5%Gd_2O_3 sintered pellets vs. Gd_2O_3 agglomerate size in powder mixture (from [4]).

Sieve fraction, mesh	Agglomerate size, μm	Whether mixture was milled	Typical pore sizes	Density, g/cm^3
−100 + 200	74 - 149	No	160, 140, 80, 40 and less	10.13
−200 + 400	37 - 74	No	80, 40 and less	10.16
−400 + 500	31 - 37	No	-	10.20
−500	31	No	30, 20 and less	10.25
−200	5 and less	Yes	5 and less	10.53
Control pellet of UO_2 without Gd_2O_3				10.59

the final compaction process and retained their form through the sintering process [24]. Pore growth as a consequence of grain growth has been demonstrated by Kingery *et al*. [25]. Kang and Yoon [26] found that the impeding effect of an entrapped gas diminishes with lower gas pressure in the sintering furnace atmosphere, with higher solid−gas interfacial tension, with smaller initial pore size and with higher dihedral angle. A narrow but fine particle size distribution is preferred in the manufacture of high performance ceramics [27]. It is therefore essential to begin with agglomerate free fine UO_2 powders in order to avoid low density associated with powder packing problems in the compaction process [28]. The difference between the theoretical density of UO_2 (10.96 g/cm^3) and its actual experimental density (10.59 g/cm^3) in **Table 3** is a useful characteristic of the UO_2 powder and is indicative of the powder packing deficiency in the compacting die.

Densification takes place uniformly without pore formation in spite of the Kirkendall effect if the void left by Gd_2O_3 agglomerate is so small as to be unstable and possesses the driving force for shrinking and closure [2]. This author had also prepared Gd_2O_3 green pellets with agglomerates of UO_2 dispersed in it. On sintering the pellet in hydrogen, it acquired a clear greenish yellow tinge compared to grayish yellow colour of an undoped Gd_2O_3 pellet indicating the ease of diffusion of uranium ions from the inside to the surface of the Gd_2O_3 pellet.

Problems originating from heterogeneous distribution of oxides are minimized in the case of sol-gel fuel due to mixing of urania and gadolinia at molecular level [29]. Restivo *et al*. [30] found that the addition of $Al(OH)_3$, SiO_2, Nb_2O_5 and TiO_2 at 0.5 wt.% as sintering aids has improved the sintered density.

5. Co-Precipitation

In course of time, powder milling had to be discontinued due to air radioactivity containment problems and increasingly stringent regulation. Co-precipitation of U and Gd is expected to provide homogeneity at atomic level by forming mixed crystals. The presence of complete solid solution of co precipitated UO_2-Gd_2O_3 is reported up to a wt.% of 30 by Wada *et al*. [31]. Hence the method was chosen as an alternative to mechanical mixing [4]. In the presence of Uranium, greater quantities of Gd get co precipitated as shown in **Table 4**.

In the experience of this author, while the powder mixture was more homogeneous in the co precipitation route, the sintered densities of the UO_2-Gd_2O_3 pellets obtained were somewhat lower than those obtained in the case of mechanical mixing and light milling route [4].

Subsequently, Riella *et al*. [32] found that the sinterability of the UO_2-Gd_2O_3 pellets obtained from dry blended powders is markedly different from that of pellets prepared by AUC-ADU co precipitation. Higher sintered densities were achieved in sample prepared following the co precipitation route. The X ray diffraction patterns of the powder samples from co precipitated UO_2-Gd_2O_3 powders show no Gd peaks, indicating that the Gd is incorporated into the UO_2 lattice in the early stages of processing. This is advantageous in sintering since single phase material always gives better results. The typical mechanical mixtures of powders always yielded pellets with lower densities.

6. Atmosphere and Additive Effects

The crystal structure of UO_2 is face centered cubic, fluorite type, with uranium atoms occupying the corners and face centers of the cube while the oxygen atoms occupy the tetrahedral interstices. UO_2 being nonstoichiometric, an exchange of oxygen between the crystal and ambient atmosphere is possible. When the ambient oxygen partial pressure (p_{O2}) is higher than the equilibrium value, oxygen enters the lattice, creating an oxygen interstitial. Since a neutral oxygen atom has to acquire electrons on being incorporated into anion lattice, holes are also created:

Table 4. Comparison of precipitation of Gd from Gd nitrate with co precipitation of Gd from (U, Gd) nitrate by NH_4OH solution, expressed as percent of Gd precipitated [6].

pH	Percent Gd precipitated	
	From Gd nitrate	From (U, Gd) nitrate
7.0	39.85	65.20
7.5	88.44	90.35
8.0	96.40	98.50
8.5	98.70	99.58

$$\frac{1}{2}O_2(g) = O_i'' + 2h^{\bullet} \quad (1)$$

Here, Kroger and Vink notation [33] has been used. The subscript i indicates interstitial position. The superscript dot indicates effective positive charge and the prime indicates effective negative charge. If two of the interstitial oxygen takes up lattice sites, a uranium site has to fall vacant:

$$O_2(g) = V_U'''' + 2O_O + 4h^{\bullet} \quad (2)$$

The effects described above may also be realized by doping UO_2 with higher valent oxide, such as Nb_2O_5. Some of the U atoms are substituted by Nb atoms and oxygen interstitials (or vacant uranium sites) are created.

$$Nb_2O_5 \xrightarrow{UO_2} 2Nb^{\bullet}_U + 4O_O + O_i''$$

$$2Nb_2O_5 \xrightarrow{UO_2} 4Nb^{\bullet}_U + 10O_O + V_U''''$$

Thus the effect of an oxidizing atmosphere is the same as that of adding a higher valency additive to UO_2 in respect of anion interstitials and cation vacancies, though the concentrations of defects in the case of additive are independent of the oxygen pressure and temperature. Matzke [34] found that the incorporation of 0.1 mol percent Nb_2O_5 increased the diffusion coefficient of Uranium by 225 times that of undoped UO_2 at 1450˚C. These phenomena (of oxygen pressure and doping) were commercially exploited in oxidative sintering at 1100˚C instead of the usual 1750˚C in reducing atmosphere. The pellets made by oxidative sintering at low temperature must, however, pass the re-sintering test at 1750˚C to ensure that there would be no in-reactor fuel densification.

When the ambient p_{O2} is low, oxygen leaves the UO_2 lattice, creating vacant oxygen sites represented by V_O:

$$O_O = \frac{1}{2}O_2(g) + V''_O + 2h^{\bullet}$$

A deficiency of oxygen is effectively the same as that of creation of uranium interstitials:

$$2O_O = O_2(g) + U_i'''' + 4h^{\bullet}$$

The effects described above may also be realized by doping UO_2 with lower valent oxide, such as Gd_2O_3.

When UO_2 is doped with lower valency additive such as Gd, some of the U atoms are substituted by Gd atoms and oxygen vacancies, denoted by V_O are created.

$$Gd_2O_3 \xrightarrow{UO_2} 2Gd^{\bullet}_U + 3O_O + V''_O$$

If no oxygen site is vacant, then there must be a uranium atom as interstitial.

$$2Gd_2O_3 \xrightarrow{UO_2} 4Gd^{\bullet}_U + 6O_O + U_i''''$$

Thus the effect of reducing ambient oxygen pressure is the same doping UO_2 with lower valency additive, though the concentrations of defects in the case of additive are again independent of the oxygen pressure and temperature.

The electrical conductivity of a nonstoichiometric oxide changes with temperature and oxygen pressure. For a particular temperature, the conductivity is expected to follow a U curve, with electron conductivity dominating at low oxygen pressures and hole conductivity dominating at high oxygen pressures. The lowest conductivity is that corresponding to stoichiometric composition of the oxide. The stoichiometric composition itself is a function of temperature. In the case of UO_2, at a temperature of 1400˚C, the stoichiometric state, as read out from the graph of Ruello *et al*. [35] corresponds to $p_{O2} = 10^{-6}$ atm. At 700˚C, the stoichimetric state corresponds to p_{O2} of the order of 10^{-24} atm.

Even in the so-called ‘reducing atmosphere’ such as hydrogen in a commercial sintering furnace, there is significant p_{O2} present in most processing conditions. Hence UO_2 may be taken to be mostly in a hyperstioichiometric state and the following possibilities of hypostoichiometric UO_2 may be taken to be of less significance:

$$O_O = \frac{1}{2}O_2(g) + V^{\bullet\bullet}_O + 2e''$$

$$2O_O = O_2(g) + U^{\bullet}_i + 4e''''$$

7. Lattice Parameter

It is known that the lattice parameter of UO_{2+x} decreases as the hyperstoichiometry is increased. Desgranges *et al*. [36] measured the expansion of a single crystal of UO_2 as a function of p_{O2} at particular temperatures. According to Equation (1) in Section 6, the oxygen interstitial formation would result in a decrease of the unit cell parameter. According to Equation (2), the new unit cell formation results in a uranium vacancy formation. The observed expansion is thought to have been induced by the formation of new unit cells. They also concluded that the concentration of oxygen interstitials is a hundred times higher than that of uranium vacancies.

Leinders *et al*. [37] determined the lattice parameter of UO_2 to be 5.47154 Å at 25˚C. Venkatakrishnan *et al*. [38] determined the lattice parameter of $(U_{1-y}Gd_y)O_{2\pm x}$ as a function of y. Hertog [39] experimentally found that the lattice parameter obeys the equation

$$d = -0.15821y + 5.47087 \tag{3}$$

McMurray [40] used the following expression for lattice parameter:

$$d = \left(4/\sqrt{3}\right)\left[yr_{Gd^{2+}} + yr_{U^{5+}} + (1-2y)r_{U^{4+}} + r_{O^{2-}}\right] \tag{4}$$

where r indicates the ionic radius. He showed that the lattice parameter calculated using the expression was in agreement with experimentally determined values of other researchers.

8. Unit Cell

Four kinds of unit cell possibilities of Gd added UO_2 are given below.

Case 1: Oxygen vacancy model for low oxygen pressures

$$GdO_{1.5} + U_3O_6 = U_3GdO_{7.5}\left(V_0\right)_{0.5}$$

Here, all of the U is in 4 valency.

Case 2: Uranium interstitial model for low oxygen pressures

$$GdO_{1.5} + U_3O_6 + U_{0.25}O_{0.5} = U_3\left(U_i\right)_{0.25}GdO_8$$

Here also, all of the U is in 4 valency.

Case 3: Uranium oxidation model with $U^{4+} \rightarrow U^{5+}$ for higher oxygen pressures

The excess Oxygen due to Gd substitution can oxidize U from 4 to 5 or 6. For every one Gd substituting for U, there can be either two U^{5+} or one U^{6+}.

$$GdO_{1.5} + U_2O_4 + UO_{2.5} = \left(U^{4+}\right)_2\left(U^{5+}\right)GdO_8$$

In the above, some of the U is in 5 valency and the remaining U is in 4 valency. It has been assumed that all Oxygen sites are filled.

Case 4: Uranium oxidation model with $U^{4+} \rightarrow U^{6+}$ for higher oxygen pressures

$$GdO_{1.5} + U_2O_4 + UO_3 = \left(U^{4+}\right)_2\left(U^{6+}\right)GdO_8\left(O_i\right)_{0.5}$$

In the above, some of the U is in 6 valency and the remaining U is in 4 valency. It has been assumed that all Oxygen sites are filled and in addition, there is interstitial oxygen to satisfy valency requirement.

In UO_2 oxidation, Andersson *et al*. [41] investigated the formation of UO_{2+x} derived from the fluorite structure by density functional theory (DFT) calculations. They found that although the transition from fluorite to the layered U_3O_8 structure occurs at U_3O_7 or $U_3O_{7.333}$, the fluorite-derived compounds are favored up to $UO_{2.5}$, that is, as long as the charge-compensation for adding oxygen atoms occurs via formation of U^{5+} ions, after which U_3O_{8-y} becomes more stable. On this basis, we may assume here that U^{5+} is more likely than U^{6+} when Gd is substituting for U in the UO_2 crystal.

9. Theoretical Density

When Gd_2O_3 is homogeneously mixed with UO_2, and sintered to form solid solution, the Gd atoms replace the position of U atoms in the fluorite crystal structure of UO_2. Since a Gd atom is lighter than a U atom, the theoretical density of (U, Gd)O_2 decreases with an increase in Gd concentration. However, this effect is partially

compensated by the reduction of the lattice parameter which tends to decrease with increase in Gd concentration [42].

The theoretical density of UO_2-Gd_2O_3 may be calculated using atomic weights and lattice parameter of the unit cell. Density is given by

$$\rho = \sum N_c A / (V_c N_A) \tag{5}$$

where N_c = the number of atoms in the unit cell, A = Atomic mass, g/mol, V_c = volume of the unit cell, cm^3 and N_A = Avagadro Number = 6.022×10^{23} atoms/g mol.

The atomic masses are taken to be 238.02891, 157.25 and 15.999 for U, Gd and O respectively.

The lattice parameter of $U_{1-y}Gd_yO_2$ is available as a function of Gd content. The unit cells presented above correspond to a Gd content $y = 0.25$. Using the expressions either 3 or 4 above, for $y = 0.25$, the lattice parameter is seen to be 5.43×10^{-8} cm.

Substituting the above values in the expression for theoretical density, the theoretical densities from unit cell calculations are seen to be 10.282, 10.982, 10.365 and 10.448 g/cm^3 for Cases 1, 2, 3 and 4 of unit cell configurations respectively. Since the experimentally determined densities decrease with Gd_2O_3 content, Case 2 is unlikely wherein the density should increase. The unit cell parameters for Cases 1 and 3 are shown in **Table 5**.

The density of UO_2-Gd_2O_3 as a function of Gd_2O_3 weight percent found in literature [43] [44] is given by

$$\rho = \rho_{UO_2} - 0.04(Gd_2O_3\%)$$

10. Green and Sintered Densities

The experimentally obtained green densities of UO_2-Gd_2O_3 for different Gd_2O_3 contents are given in **Figure 2**. The corresponding sintered densities are given in **Figure 3**.

The estimated density of UO_2-Gd_2O_3 versus Gd_2O_3 wt.% for a UO_2 density of 10.59 g/cm^3 corresponding to Cases 1 and 3 is shown in **Figure 4** along with experimentally determined values.

Table 5. Unit cell parameters of UO_2-Gd_2O_3.

	Case 1	Case 3
Unit cell composition	$(U^{4+})_3GdO_{7.5}(V_0)_{0.5}$	$(U^{4+})_2(U^{5+})GdO_8$
Unit cell mass	991.32923	999.32873
Gd oxide mass	181.2485	181.2485
Wt.% Gd oxide	18.2834	18.1370
Theoretical density, g/cm^3	$\rho = 10.96 - 0.037(Gd_2O_3\%)$	$\rho = 10.96 - 0.033(Gd_2O_3\%)$
Actual density, g/cm^3	$\rho = \rho_{UO_2} - 0.037(Gd_2O_3\%)$	$\rho = \rho_{UO_2} - 0.033(Gd_2O_3\%)$

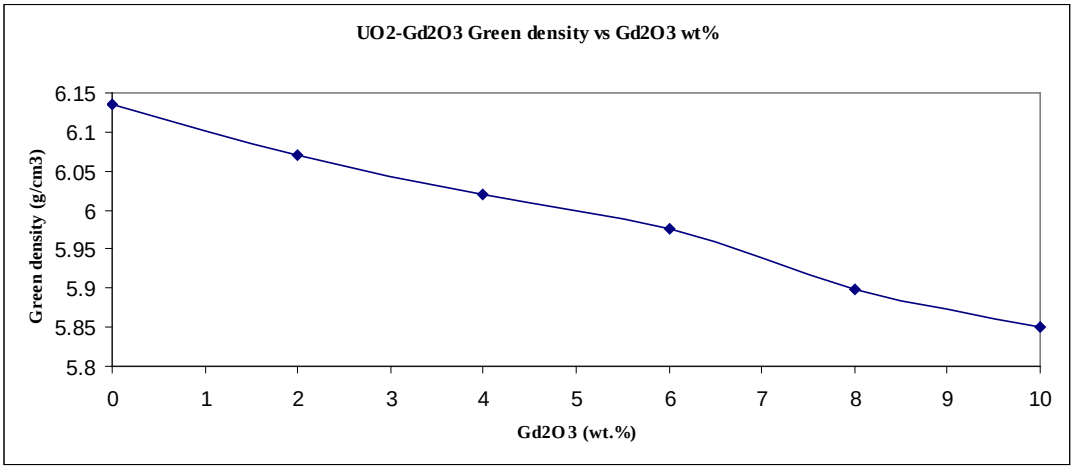

Figure 2. Green density of UO_2-Gd_2O_3 versus Gd_2O_3 content using data from [6].

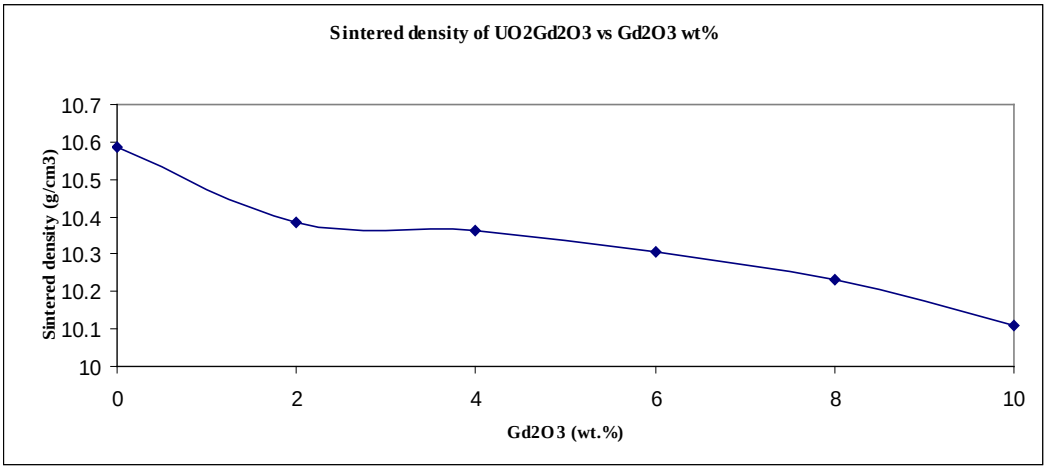

Figure 3. Sintered density of UO_2-Gd_2O_3 versus Gd_2O_3 content, using data from [6].

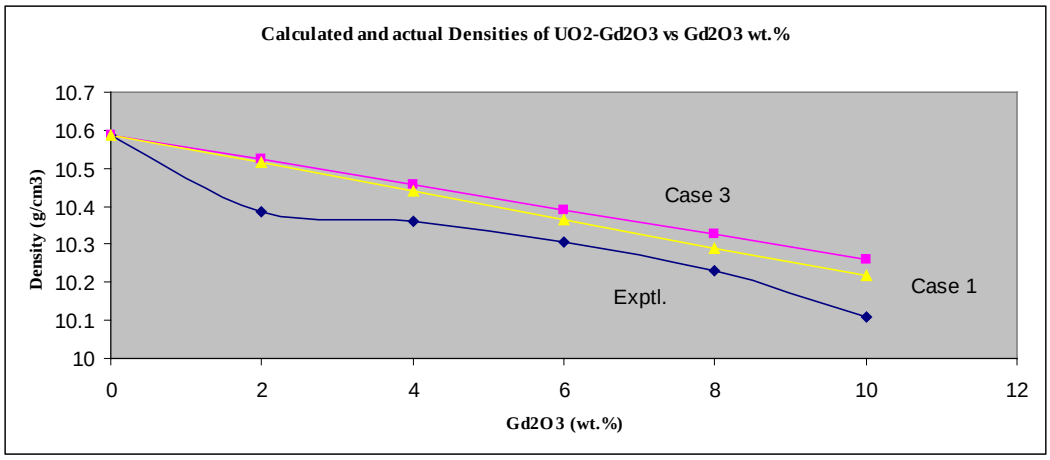

Figure 4. Calculated and experimental densities of UO_2-Gd_2O_3 versus Gd_2O_3 content.

The actual density of UO_2-Gd_2O_3 is found to be less than that calculated using the expressions:

$\rho = \rho_{UO_2} - 0.037(Gd_2O_3\%)$ for Case 1.

$\rho = \rho_{UO_2} - 0.033(Gd_2O_3\%)$ for Case 3.

This shows that the agglomerate effect of Gd_2O_3 was only partially mitigated in the manufacturing process followed.

11. Diffusion

In UO_2, it is the uranium ion that moves slowly in the cation lattice relative to the oxygen ion in the anion lattice. To maintain electrical neutrality, however, both cation and anion have to move in tandem. Hence cation diffusion becomes rate controlling in diffusion dependent processes such as sintering and creep. Any step aimed at speeding up the cation will also speed up sintering and creep.

Matzke [45] underlined the relationship between the point defects in UO_2. Higher valent cations, substituting for U^{4+} ions in the UO_2 lattice, impart an effective positive charge to the lattice. This leads to the decrease of the concentration of oxygen vacancies and then to the increase of the concentration of oxygen interstitials through Frenkel defect equilibrium, thereby increasing the concentration of cation vacancies through Schottky defect equilibrium. The increase of the concentration of cation vacancies is expected to cause the increase of the self diffusion coefficients of Uranium.

On the other hand, lower valent cations, substituting for U^{4+} ions in the UO_2 lattice, impart an effective nega-

tive charge to the lattice. This leads to the increase of the concentration of oxygen vacancies and then to the decrease of the concentration of oxygen interstitials through Frenkel defect equilibrium, thereby decreasing the concentration of cation vacancies through Schottky defect equilibrium. The decrease if the concentration of cation vacancies is expected to cause the decrease of the self diffusion coefficients of Uranium. The ratios of diffusion coefficients of doped to undoped UO_2 are given in **Table 6**.

As already stated, the concentration of uranium vacancies is enhanced by increasing the oxygen partial pressure in the ambient atmosphere or by the incorporation of a higher valency additive such as Nb. On the other hand, the concentration of oxygen vacancies is increased by the incorporation of a lower valency additive such as Gd. The concentration of oxygen vacancies caused by the substitution of U by Gd will depend on the amount of Gd added to the uranium, two Gd ions yielding one oxygen vacancy.

Manzel and Dorr [46] found that the addition of some percent of Gd_2O_3 to UO_2 has a pronounced effect on the sintering behaviour. Above 1200˚C, the shrinkage of the UO_2-Gd_2O_3 pellet was delayed because of the start of the formation of solid solution.

In the expression for the diffusion

$$D\left(\mathrm{cm}^2/\mathrm{s}\right) = D_0 \exp\left[-Q\left(\mathrm{eV}\right)/kT\right]$$

Some uranium ion diffusion coefficients and a gadolinium ion diffusion coefficient in UO_2 from literature [47]-[51] are given in **Table 7**. For ease of comparison, the calculated **D** values at 1500˚C are included. Gd is seen to move much more slowly than U in UO_2.

Hence, with the incorporation of Gd in the UO_2 lattice, a slow down in sintering is normally expected, being a diffusion related process. However, the anticipated slow down in sintering was not noticed in the UO_2-1.5%Gd_2O_3 pellet production experience by this author using industrial sintering furnaces. The same pusher type hydrogen atmosphere sintering furnaces used for sintering UO_2 were also used for sintering UO_2-Gd_2O_3. No significant difference in sintering behaviour could be noticed. The dew point of the hydrogen was −30˚C to −40˚C in which range UO_2 is hyperstoichiometric. The steep increase in diffusion (from the order of 10^{-17} to 10^{-13} as x in UO_{2+x} is increased (from 2.00 to 2.05) at 1500˚C is well established [34]. At 1500˚C, Matzke [52] gives the equation $\log D = -10.85 + 1.5 \log x$.

The decrease in the concentration of uranium vacancies caused by substituting Gd for U to a small extent (1.5% Gd_2O_3 in the mixture) is perhaps more than made up by the significant p_{O2} normally present in commercial reducing sintering atmospheres. This view is supported by the work of Une [53] who determined the grain boundary diffusion coefficients for UO_2, UO_2-5wt.% Gd_2O_3 and UO_2-10wt.% Gd_2O_3 as a function of oxygen potential in the range −500 to −250 kJ/mol, corresponding to O/U change from 2.000 to 2.005. At a low oxygen potential of −500 kJ/mol or O/U of 2.000, the grain boundary diffusion coefficient was found to decrease as the Gd_2O_3 content is increased. However, the diffusion coefficients merged to an almost single value at higher oxygen potential of about −250 kJ/mol corresponding to O/U of 2.005. Even in the reducing atmosphere of an industrial sintering furnace (H_2 or cracked ammonia), the oxygen pressure is usually sufficiently high to maintain

Table 6. Ratio of Diffusion coefficient of U in 0.1 mole% doped UO_2 to that in undoped UO_2, Matzke [45].

Material	D_{doped}/D_{pure}	
	1673 K	1823 K
UO_2 +La_2O_3	~0.02	0.085
UO_2 + Y_2O_3	~0.02	0.11
UO_2 + Nb_2O_5	225	1

Table 7. Pre exponential term, activation energy and D_{1500} for self diffusion of U and Gd in UO_2.

Cation	D_0	Q, ev	Temperature	Reference	D at 1500˚C
U	4.0×10^{-7}	3.0	1477˚C - 1720˚C	**48**	1.196×10^{-15}
U	5.82×10^{-5}	3.2	1900˚C - 2150˚C	**49**	4.697×10^{-14}
U	2.04×10^{-3}	3.9	1400˚C - 1650˚C	**50**	1.689×10^{-14}
Gd	5.3×10^{-3}	5.1	1500˚C - 1703˚C, H_2	**51**	1.707×10^{-17}

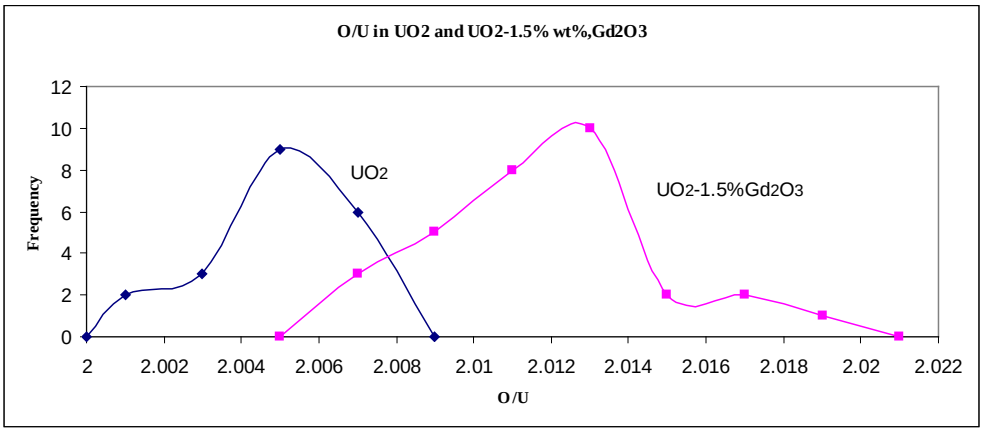

Figure 5. Frequency distributions of O/U in UO_2 and UO_2−1.5%Gd_2O_3.

UO_2 in hyper-stoichiometric state. The volume diffusion coefficient follows the same trend, though being much smaller than the grain boundary diffusion coefficient.

12. U^{6+} and Gd Content

Samples of UO_2 and UO_2−1.5%Gd_2O_3 sintered pellets were dissolved in H_2SO_4 solution (containing a little HF). Any U^{5+} present in the sample disproportionates to U^{4+} and U^{6+} upon dissolution. The concentrations were determined by polarography. As Gd_2O_3 is relatively nonstoichiometric, an increase in the ratio O/U is indicative of the extent of oxidation of U^{4+} to higher valency in the solid state. **Figure 5** shows the frequency distributions of O/U ratios of UO_2 and UO_2-1.5%Gd_2O_3 sintered pellets obtained in this author's work in one production campaign.

For UO_2, the frequent value of O/U in **Figure 5** is 2.005 while for UO_2-1.5%Gd_2O_3, it is 2.013. In other words, the U^{6+} in solutions prepared by dissolving UO_2-1.5%Gd_2O_3 is higher than that from UO_2. The higher U^{6+} is indicative of the presence of U^{5+} in the solid solution, corresponding to Case 3 rather than Case 1 in section 8 above. The presence of U^{6+} in UO_2 even when not containing UO_2-Gd_2O_3 is indicative of the dominance of oxygen interstitials over oxygen vacancies and prevalence of an overall oxidative condition in a hydrogen atmosphere furnace.

13. Summary and Conclusion

Unfavourable powder characteristics (such as a strong tendency to agglomerate) and small proportions (1.5 wt.%) made Gd_2O_3 powder difficult to disperse uniformly in UO_2 powder, necessitating the use of a suitable mixing machine. Formulas based on mean and standard deviation of analytical sample results were used to compare the efficiencies of mixing machines. The powder mixture had to be lightly milled to ensure a small particle size of Gd_2O_3 dispersed in the powder mixture. This in turn led to quick dissolution of the Gd_2O_3 and closure of the void formed on dissolution during sintering. Densification took place uniformly without pore formation in spite of the Kirkendall effect if the void left by Gd_2O_3 agglomerate was small enough to be unstable and shrink further to close. Alternatively, the Gd could be incorporated in UO_2 by co-precipitation, though with the possibility of slightly lower sintered densities. The actual sintered densities obtained were lower than those calculated for different unit cell models, pointing to the partially unmitigated effect of Gd_2O_3 agglomerates. The lower diffusivities expected on Gd addition did not appear to have any significant effect on sinterability in pellet manufacture by this author. This may probably be due to the predominance of effects of p_{O2} over that of doping at small levels. Slow down of sintering of UO_2-Gd_2O_3 pellets may be attributed more to larger sized agglomerate of Gd_2O_3 powder than to lower valency additive effects or to dissolution interfering with densification.

Acknowledgements

Thanks are due to my erstwhile doctoral student Dr. B. Narasimha Murty, Nuclear Fuel Complex, Hyderabad, India for his useful discussion.

References

[1] Balakrishna, P., Narayanan, P.S.A, Somayajulu, G.V.S.R.K. and Sinha, K.K. (1977) Special Features in the Fabrication of Mixed Oxides. *Transactions of the Powder Metallurgy Association of India*, **4**, 25-31.

[2] Balakrishna, P., Narayanan, P.S.A., Somayajulu, G.V.S.R.K. and Sinha, K.K. (1979) Fabrication of Burnable Poison Fuel Pellets for TAPS—Plant Experience. *Symposium on Sintering and Sintered Products*, Bhabha Atomic Research Centre, Bombay, October 29-31 1979, 401-421.

[3] Balakrishna, P., Somayajulu, G.V.S.R.K., Sinha, K.K. and Kondal Rao, N. (1979) Special Features in Sintering UO_2-Gd_2O_3 Compacts. *Transactions of the Powder Metallurgy Association of India*, **6**, 80-89

[4] Balakrishna, P., Nandi, D., Narayanan, P.S.A. and Somayajulu, G.V.S.R.K. (1986) Investigation of Alternative Routes for Producing UO_2-Gd_2O_3 Mixed Oxide for Nuclear Fuel Applications. In: Ramanujam, M., Ed., *Advances in particulate Technology, Proceedings of the International symposium on "Recent Advances in Particulate Technology"*, I.I.T. Madras, Chennai, 8-10 December 1982,.

[5] Balakrishna, P., Narayanan, P.S.A., Somayajulu, G.V.S.R.K. and Varma, B.P. (1986) Fabrication of UO_2 (U,Gd)O_2 and ThO_2 Pellets, a View Point. *Transactions of the Powder Metallurgy Association of India*, **13**, 63-67.

[6] Balakrishna, P., Kulkarni, A.P., Somayajulu, G.V.S.R.K., Swaminathan, N. and Balaramamoorthy, K. (1991) Sintering UO_2-Gd_2O_3. In: Vincenzini, P., Ed., *Ceramics Today—Tomorrow's Ceramics*, Elsevier Science Publishers B.V., Amsterdam.

[7] Balakrishna, P., Kulkarni, A.P., Krishnan, T.S., Balaramamoorthy, K., Ramamohan T. and Ramakrishnan, P. (1992) Retarded Densification and Desintering in Ceramic Bodies, In: Ramakrishnan, P., Ed., *Advanced Ceramics*, Oxford & IBH Publishing Co., New Delhi, 67-76.

[8] Balakrishna, P., Kartha, R.M. and Ramakrishnan, P. (1993) Sintering of Co-Precipitated Ceramic Mixtures. *Transactions of the Powder Metallurgy Association of India*, **20**, 41-48.

[9] ASTM C922-14 Standard Specification for Sintered Gadolinium Oxide-Uranium Dioxide Pellets.

[10] ASTM C968-12 Standard Test Methods for Analysis of Sintered Gadolinium Oxide-Uranium Dioxide Pellets.

[11] Matzke, H.J. (1966) On the Effect of TiO_2 Additions on Defect Structure, Sintering and Gas Release of UO_2. AECL, 2585,

[12] Ainscough, J.B., Rigby, F. and Osborn, S.C. (1974) The Effect of Titania on Grain Growth and Densification of Sintered UO_2. *Journal of Nuclear Materials*, **52**, 191-203. http://dx.doi.org/10.1016/0022-3115(74)90167-6

[13] Heal, T.J., Littlechild, J.E. and Watson, R.M. (1973) Development of Stable Density UO_2 Fuel. In: John, C.T., Wyles, B. and Moore, B., Eds., *Nuclear Fuel Performance, Proceedings of International Conference*, British Nuclear Energy Society, London, 15-19 October 1973, Paper No. 52.

[14] Pope, J.M. and Radford, K.C. (1976) Stable Reactor Fuel of Controlled Density Using Active UO_2 Powders. *Materials Research Bulletin*, **11**, 585-592.

[15] Radford, K.C. and Pope, J.M. (1977) Controlled Porosity Reactor Fuel. *Journal of Nuclear Materials*, **64**, 289-299. http://dx.doi.org/10.1016/0022-3115(77)90081-2

[16] Davis, H.H. and Potter, R.A. (1978) UO_2-Gd_2O_3 Sintering Behaviour. In: Palmer, H., Davis, R.F. and Hare, T.M., Eds., *Processing of Crystalline Ceramics*, Materials Science Research, Vol. 11, Plenum Press, New York, 515-524

[17] Song, K.W., Kim, K.S., Yoo, H.S. and Jung, Y.H. (1998) Effect of UO_2 Powder Property and Oxygen Potential on Sintering Characteristics of UO_2-Gd_2O_3 Fuel. *Journal of Korean Nuclear Society*, **30**, 128-139.

[18] Song, K.W., Kim, K.S., Yang, J.H., Kang, K.W. and Jung, Y.H. (2001) A Mechanism for the Sintered Density Decrease of UO_2-Gd_2O_3 Pellets under an Oxidizing Atmosphere. *Journal of Nuclear Materials*, **288**, 92-99. http://dx.doi.org/10.1016/S0022-3115(00)00721-2

[19] Nishida, T. and Yuda, R. (1998) Effect of Particle Size and Oxygen Potential on UO_2-Gd_2O_3 Pellet Sintering, Advances in Fuel Pellet Technology for Improved Performance at High Burnup. *Proceedings of Technical Committee Meeting, IAEA TECH DOC*, 1036, 73-84.

[20] Ho, S.M. and Radford, K.C. (1986) Structural Chemistry of solid Solutions in the UO_2-Gd_2O_3 System. *Nuclear Technology*, **73**, 350-360.

[21] Durazzo, M. and Riella, H.G. (2010) The Sintering Blockage Mechanism in the UO_2-Gd_2O_3 System. *Proceedings of the Transactions of the European Nuclear Conference*, Barcelona, 30 May-2 June 2010, 4-10.

[22] Durazzo, M., Saliba-Silva, A.M., Urano de Carvalho, E.F. and Riella, H.G. (2013) Sintering Behavior of UO_2-Gd_2O_3 Fuel: Pore Formation Mechanism. *Journal of Nuclear Materials*, **433**, 334-340. http://dx.doi.org/10.1016/j.jnucmat.2012.09.033

[23] Song, K.W., Lee, Y.W., Yang, M.S., Sohn, D.S. and Kang, Y.H. (1994) Pore Growth in Sintered UO_2. *Journal of Nuclear Materials*, **209**, 263-269. http://dx.doi.org/10.1016/0022-3115(94)90261-5

[24] Chalder, G.H. (1962) The Properties of Active Ceramic Oxide Powders in Relation to Sintering Behaviour. In: Knepper, W.A., Ed., *Agglomeration*, Interscience Publishers, New York, 111-114.

[25] Kingery, W.D., Bowen, H.K. and Uhlmann, D.R., Eds. (1976) Introduction to Ceramics. 2nd Edition, John Wiley, New York.

[26] Kang, S.J.L. and Yoon, K.J. (1989) Densification of Ceramics Containing Entrapped Gases. *Journal of the European Ceramic Society*, **5**, 135-139. http://dx.doi.org/10.1016/0955-2219(89)90020-4

[27] Barringer, E., Jubb, N., Fegley, B., Pober, R.L. and Bowen, H.K. (1984) Processing Monosized Powders. In: Hench, L.L. and Ulrich, D.R., Eds., *Ultrastructure Processing of Ceramics, Glasses and Composites*, John Wiley and Sons, New York, 315-333.

[28] Balakrishna, P., Singh, A. and Sinha, K.K. (1997) Agglomerate Free Fine UO_2 Powders. *Proceedings of the International Conference, TOPFUEL'*97, Manchester, 9-11 June 1997, 98-103.

[29] Gunduz, G. and Uslu, I. (1996) Powder Characteristics and Microstructure of Uranium Dioxide and Uranium Dioxide-Gadolinium Oxide Fuel. *Journal of Nuclear Materials*, **231**, 113-120. http://dx.doi.org/10.1016/0022-3115(96)00349-2

[30] Restivo, T.A.G., Cláudio, A.E.L., Silva, E.D. and Pagano Jr., L. (2003) Effect of Additives on the Sintering Kinetics of the $UO_2Gd_2O_3$ System. *Proceedings of a Technical Committee Meeting*, Brussels, 20-24 October 2003, 147-153.

[31] Wada, T., Noro, K. and Tsukui, K. (1973) Behaviour of UO_2-Gd_2O_3 Fuel. In: John, C.T., Wyles, B. and Moore, B., Eds., *Nuclear Fuel Performance*, British Nuclear Energy Society, London, 63.1-63.3.

[32] Riella, H.G., Durazzo, M., Hirata, M. and Nogueira, R.A. (1991) UO_2-Gd_2O_3 Solid Solution Formation from Wet and Dry Processes. *Journal of Nuclear Materials*, **178**, 204-211. http://dx.doi.org/10.1016/0022-3115(91)90387-M

[33] Kröger, F.A. and Vink, H.J. (1956) Relations between Concentrations of Imperfections in Crystalline Solids. In: Seitz, F. and Turnbull, D., Eds., *Solid State Physics*, Volume 3, Academic Press, New York, 307-435.

[34] Matzke, H.J. (1982) Application of Diffusion Results in Technology: Increased Uranium Self Diffusion in UO_{2+x} and $(U,Nb)O_{2+x}$. European Institute for Transuranium Elements, Report EUR-7700.

[35] Ruello, P., Petot-Ervas, G., Petot, C. and Desgranges, L. (2005) Electrical Conductivity and Thermoelectric Power of Uranium Dioxide. *Journal of the American Ceramic Society*, **88**, 604-611. http://dx.doi.org/10.1111/j.1551-2916.2005.00100.x

[36] Desgranges, L., Gramond, M., Petot, C., Petot-Ervas, G., Ruello, P. and Saadi, B. (2005) Characterisation of Uranium Vacancies in Hyper Stoichiometric Uranium Dioxide. *Journal of the European Ceramic Society*, **25**, 2683-2686. http://dx.doi.org/10.1016/j.jeurceramsoc.2005.03.123

[37] Leinders, G., Cardinaels, T., Binnemans, K. and Verwerft, M. (2015) Accurate Lattice Parameter Measurements of Stoichiometric Uranium Dioxide. *Journal of Nuclear Materials*, **459**, 135-142. http://dx.doi.org/10.1016/j.jnucmat.2015.01.029

[38] Venkata Krishnan, R., Panneerselvam, G., Manikandan, P., Antony, M.P. and Nagarajan, K. (2009) Heat Capacity and Thermal Expansion of Uranium-Gadolinium Mixed Oxides. *Journal of Nuclear and Radiochemical Sciences*, **10**, 19-26.

[39] Hertog, J. (2011) Lattice Parameter Evolution of Single Doped and Co-Doped UO_2 Systems. External Report of the Belgian Nuclear Research Centre, SCK-CEN-ER-175.

[40] McMurray, J.W. (2014) Thermodynamic Modeling of Uranium and Oxygen Containing Ternary Systems with Gadolinium, Lanthanum, and Thorium. Doctoral Dissertation, University of Tennessee, Knoxville.

[41] Andersson, D.A., Baldinozzi, G., Desgranges, L., Conradson, D.R. and Conradson, S.D. (2013) Density Functional Theory Calculations of UO_2 Oxidation: Evolution of UO_{2+x}, U_4O_{9-y}, U_3O_7, and U_3O_8. *Inorganic Chemistry*, **52**, 2769-2778. http://dx.doi.org/10.1021/ic400118p

[42] Massih, A.R., Persson, S. and Weiss, Z. (1992) Modelling of $(U,Gd)O_2$ Fuel Behaviour in Boiling Water Reactor. *Journal of Nuclear Materials*, **188**, 323-330. http://dx.doi.org/10.1016/0022-3115(92)90492-4

[43] Characteristics and Use of Urania Gadolinia Fuels, 3. Fuel Manufacturing, IAEA TECDOC-844, 50-58.

[44] International Atomic Energy Agency (1991) Guidebook on QC of MOX and Gd Bearing Fuels. IAEA-TECDOC-584.

[45] Matzke, H.J. (1966) Diffusion in Doped UO_2. *Nuclear Applications*, **2**, 131.

[46] Manzel, R. and Dorr, W.O. (1980) Manufacturing and Irradiation Experience with UO_2-Gd_2O_3 Fuel. *Ceramic Bulletin*, **59**, 601-603 & 616.

[47] Vollath, D. (1986) Uranium Self Diffusion. In: Hassce, V., Keller-Rudek, H., Manes, L., Schulz, B., Schumacher, G., Vollath, D. and Zimmermann, H., Eds., *Gmelin Handbook of Inorganic Chemistry* (*U-Uranium, Supplement*), 8th Edition, Springer-Verlag, Berlin Heidelberg, 113-118.

[48] Alcock, C.B., Hawkins, R.S., Hills, A.W.D. and Mc Namara, P. (1966) A Study of Cation Diffusion in Stoichiometric $U0_2$ Using α-Ray Spectrometry. *Thermodynamics*, **2**, 57-72.

[49] Yajima, S., Furuya, T. and Hirai, H. (1966) Lattice and Grain-Boundary Diffusion of Uranium in UO_2. *Journal of Nuclear Materials*, **20**, 162-170. http://dx.doi.org/10.1016/0022-3115(66)90004-3

[50] Hawkins, R.J. and Alcock, C.B. (1968) A Study of Cation Diffusion in UO_{2+x} and ThO_2 Using α-Ray Spectrometry. *Journal of Nuclear Materials*, **26**, 112-122. http://dx.doi.org/10.1016/0022-3115(68)90162-1

[51] Ferraz, W.B. and Sabioni, A.C.S. **(**2006) Diffusion of Gadolinium in the UO_2 Nuclear Fuel. *Cerâmica*, **52**, 143-148. http://dx.doi.org/10.1590/S0366-69132006000300006

[52] Matzke, H.J. (1969) On U Self Diffusion in UO_2 and UO_{2+x}. *Journal of Nuclear Materials*, **30**, 26-35. http://dx.doi.org/10.1016/0022-3115(69)90165-2

[53] Une, K. (1988) Effect of Oxygen Potential on the Initial Sintering of UO_2 and UO_2-Gd_2O_3 Compacts. *Journal of Nuclear Materials*, **158**, 210-216. http://dx.doi.org/10.1016/0039-9140(91)80114-F